Structure and superconductivity of Nb-Zr thin films

1989 J. Phys.: Condens. Matter 1 6685

(http://iopscience.iop.org/0953-8984/1/37/015)

J. Phys.: Condens. Matter **1** (1989) 6685–6693. Printed in the UK

Structure and superconductivity of Nb–Zr thin films

A Cavalleri†, F Giacomozzi†, L Guzman† and P M Ossi‡

† Istituto per la Ricerca Scientifica e Tecnologica, 38050 Povo (TN), Italy

‡ Istituto di Ingegneria Nucleare, Centro Studi Nucleari Enrico Fermi, Politecnico di Milano, Via Ponzio 34/3, 20133 Milano, and Unità Centro Interuniversitario Struttura della Materia (Ministero Pubblica Istruzione) di Trento, 38050 Povo (TN), Italy

Received 23 May 1988, in final form 31 January 1989

Abstract. Structural, microstructural and superconducting characteristics of Nb–Zr thin films of composition near $Nb_{80}Zr_{20}$ have been investigated by various techniques with specific attention to the influence of sample preparation technique and of the nature and temperature of the substrate.

Alloys sputter deposited at room temperature are crystalline, while those prepared at low temperatures may be amorphous depending on the deposition parameters. Multilayered samples have been implanted with N_2^+ or Kr^+ ions at various doses. Only Kr^+ ions were able to induce glass formation, which was observed to depend critically on the dose. The results obtained are discussed in the light of a recent model of glass formation in irradiated films. Both for crystalline and for amorphous alloys, T_c measurements were performed using a resistance method.

1. Introduction

The search for alloys with a relatively high superconducting transition temperature T_c has demonstrated that good candidate materials should have a high electronic density of states at the Fermi energy, resulting in a high electron–phonon coupling constant λ, a relevant electron–phonon interaction and a low average phonon frequency. However, difficulties exist in preparing alloys with a high T_c, because of the connected crystal lattice instability frequently occurring in such systems. In particular, when group V metals, with an intrinsic limited stability of the BCC structure, are alloyed with HCP elements from group IV, structural instabilities are observed at a mean number N_e of valence electrons per atom of about 4.7. On the contrary, it is simply the reduction in stability of the crystal structure that is responsible for the increase in T_c in such transition-metal solid solutions. These systems are far from the early–late-transition-metal alloys, which are recognised as being readily amorphisable. However, the presence of a lattice instability indicates that in these alloys the transition from crystalline to glassy state could be explored, thus opening the possibility of investigating superconducting behaviour in a different family of amorphous systems.

BCC bulk crystalline $Nb_{1-x}Zr_x$ presents one of the most interesting T_c trends with composition. A maximum T_c-value of about 10.7 K, higher than the T_c of pure Nb, is observed for $x = 0.25$ [1]. The system is substitutional, with a continuous series of disordered solutions; in addition to its intrinsic structural instability, the presence of a miscibility gap in the phase diagram [2] and the assessed preferential diffusivity of Zr into Nb [3] are also factors potentially favouring amorphisation.

0953-8984/89/376685 + 09 $02.50

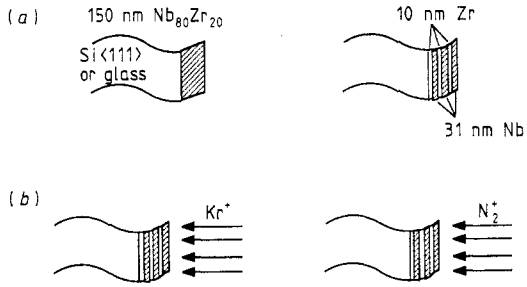

Figure 1. Schematic representation of the different sample configurations adopted. (*a*) Sputter-deposited samples. (*b*) Sputter-deposited and ion-implanted samples.

Superconductivity in highly disordered or amorphous transition-metal binary alloys poses some puzzling questions. First, the so-called Collver–Hammond [4] curve relating the variation in the highest T_c-value to the N_e ratio, which presents a single broad maximum centred around 6.4 electrons per atom for 4d metal alloys, is unexplained. Secondly, both microstructural observations [5, 6] and tunnelling data [7] show increased λ-values and a higher T_c for non-transition metals with respect to their crystalline counterparts. The tendency to obtain strong-coupling superconductivity appears to be a universal feature accompanying the onset of disorder.

Instead, for transition-metal amorphous alloys, experiments on heat capacity changes at T_c are better described within the BCS weak-coupling scheme [8]. Indeed, the values of $2\Delta/k_BT_c$ for this class of materials always approaches the weak-coupling value of 3.5 [9]. Thus, when studying inter-transition-metal alloys, we expect to be in the field of BCS superconductivity. However, contrasting trends of T_c variation with grain size were found [10], leading us to conclude that the intrinsic properties of such systems are complex and still not completely clarified. Controversy exists also concerning the role of gas impurities, often incorporated in the samples (usually thin films) by the various deposition techniques used to obtain glassy phases; such impurities are reported not to affect T_c in amorphous alloys [11] or on the contrary to depress it strongly [12].

Clarification of some of the above questions may help us to choose the best preparation technique for obtaining glassy transition-metal alloys with optimal superconducting properties. In this paper we study Nb–Zr films, prepared by different techniques, which we characterise with respect to the structural, the compositional and the superconducting properties.

2. Structural investigations

In figure 1 are schematised the various sample configurations used: the composition was centred around $Nb_{80}Zr_{20}$. Films of thickness in the 100 nm range were sputter deposited either at room temperature or at 77 K onto different (Si⟨111⟩ and glass) substrates; after deposition, some samples were implanted with 170 keV N_2^+ ions (2.5×10^{17} cm^{-2}) or Kr^+ ions (7×10^{15}, 1×10^{16} and 2.5×10^{16} cm^{-2}), taking care that the temperature never exceeded 373 K. A typical pressure value during the implantation process was 2×10^{-4} Pa. Details of the preparation procedure have been reported elsewhere [13].

Characterisation of the samples was provided by glancing as well as normal incidence x-ray diffraction (XRD), Auger electron spectroscopy (AES) complemented by secondary-ion mass spectrometry (SIMS) and scanning electron microscopy connected with energy-dispersive spectroscopy.

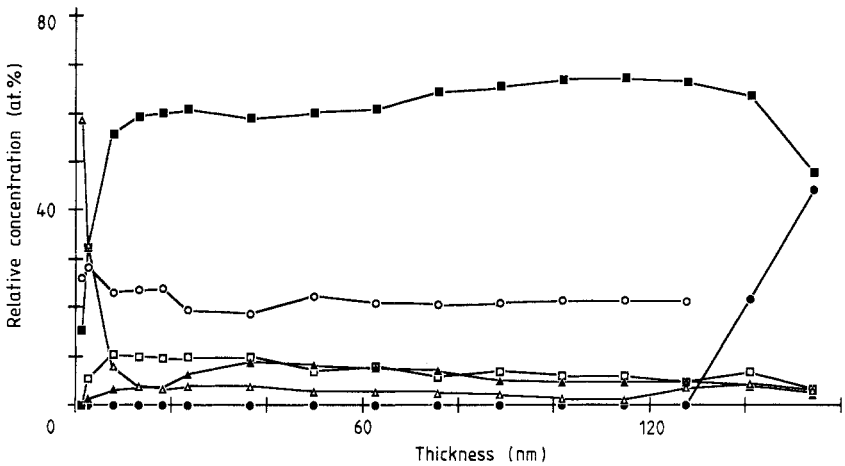

Figure 2. Compositional profile (AES) of a $Nb_{80}Zr_{20}$ sample co-sputtered at liquid nitrogen temperature on a Si substrate: ●, Si; ○, Zr; ■, Nb; □, C; ▲, N; △, O.

The film composition fits the optimal $Nb_{80}Zr_{20}$ stoichiometry very nearly; in figure 2 the compositional depth profile of a liquid-N co-sputtered sample shows also the presence of unavoidable gas contaminants (C and O), whose concentration is maintained within the reported values for all films, thus appearing to be independent of the deposition temperature; note that AES probably overestimates the C concentration [14].

The films deposited at room temperature are crystalline; the position of the Bragg peaks in the x-ray patterns reveals attainment of a solid solution. By contrast, samples prepared at low temperatures are crystalline or amorphous depending on firstly the nature of the substrate (films deposited onto glass are crystalline) and secondly the concentration of gas impurities during the process. Indeed SIMS spectra show the effectiveness of both C and O in stabilising metastable highly disordered configurations in Nb–Zr alloys, in agreement with the recent observation of the role of gas impurities in the amorphisation process [12]. We believe that the reason that it is impossible to obtain amorphous alloys when using glass substrates depends on the lower thermal conductivity and on the greater thickness of such substrates with respect to Si substrates. This results in weaker heat flow from substrate to the liquid–thermal bath and thus in a lower efficiency required to dissipate the energy deposited onto the film surface during sputtering. Indeed, for glass substrates, the effective substrate temperature is presumably higher than for Si substrates but sufficient, however, to inhibit amorphisation. In figures 3(*a*) and 3(*b*), we give the x-ray profiles for the amorphous phase and after recrystallisation at 673 K of a film co-sputtered at liquid-N temperature, respectively. Note that the second-order diffraction features in the pattern (figure 3(*a*)) can be unambiguously attributed to a glassy phase.

Multi-layered samples were ion mixed at room-temperature using both light N_2^+ and massive Kr^+ ion projectiles, thus causing different elementary defect production and interaction processes within the matrix. The good quality of the multi-layers is confirmed by the sharp Nb–Zr interfaces in the as-deposited films. The Zr diffusion into Nb already observed [3] is very limited. We should comment (compare figures 4(*a*), 4(*b*) and 4(*c*) with each other) that the AES profiles of gaseous impurities remain significantly in phase with the Zr layers; thus, while the good mixing efficiency is demonstrated by interface broadening and eventually by related reduction in periodicity in layer profiles, we do not observe uniform spreading of impurities over the mixed region. Also we note that

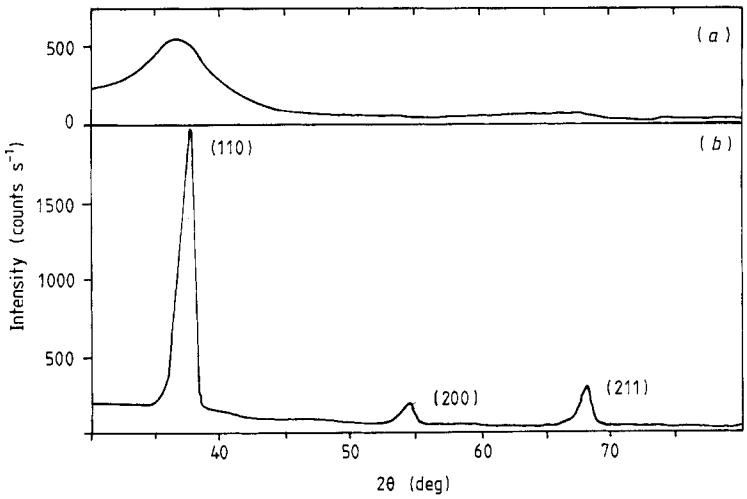

Figure 3. X-ray profiles of (*a*) an amorphous film deposited at liquid-nitrogen temperature onto a Si substrate (the arrows indicate second-order diffraction features) and (*b*) after annealing the same sample at 673 K.

the maximum C, N and O impurity contents of the order of 10 at.%, as indicated by AES, are probably overestimated. This is the limit of the quantification method based on the sensitivity factor to convert peak-to-peak ratios into absolute concentrations. Anyway we exclude formation of interstitial compounds (e.g. oxycarbon nitride), which are not revealed by XRD, but these precipitates may be present in spatially non-uniform samples.

The quite low mixing efficiency of N_2^+ ions is confirmed by the maintained periodicity of the layers after implantation at a dose which is near the highest possible in order to avoid precipitation within the matrix of nitrides; the effect of this is to depress T_c strongly, besides changing the very nature of the material. Moreover, such a light projectile is unable to produce and to stabilise a density of defects sufficient to amorphise the alloy formed in the immediate neighbourhood of the Nb–Zr interfaces (see figures 4(*a*), 4(*b*) and 5(*a*)).

Kr^+ ion implantation is much more efficient in inducing mixing of the films. In figure 4(*c*), only a weak trace of layer periodicity upon bombardment at 5×10^{16} Kr^+ cm^{-2} remains. Mixing is complete and extends far from the interface with increasing dose. The structural changes of the samples, however, at first sight may appear quite surprising. Indeed, XRD profiles show (figure 5(*b*)) the appearance of a glassy phase at Nb–Zr interfaces in films bombarded at 7×10^{15} Kr^+ cm^{-2}, while implantation at higher doses results in a crystalline solid solution, approaching a defective limit of the as-deposited co-sputtered alloys (figure 5(*c*)). The existence of a critical ion dose to amorphise the Nb–Zr periodic multi-layer confirms that this alloy belongs to the class of hard glass-forming alloys [15]; indeed in such systems, which often present spatially non-uniform amorphisation, it was observed that over-irradiation leads to destabilisation of the amorphous structure and to precipitation of crystalline products. In figure 5(*d*), we show also, for comparison, a diffraction pattern from an as-deposited Nb–Zr multi-layer.

The above structural findings give support to a recent model of bombardment-induced formation of glassy phases in binary alloys [16]. Without presenting the details of the model, the essential ideas are that the composition of the interface between energy spikes produced within the target by incoming massive ions and the surrounding lattice,

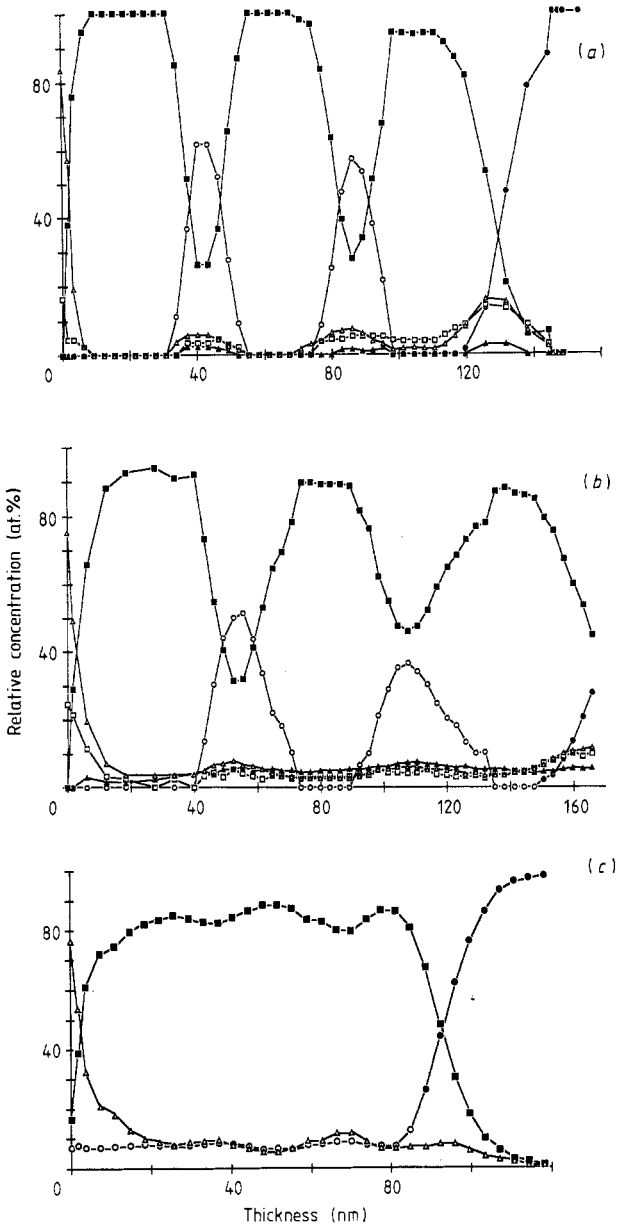

Figure 4. Compositional profiles (AES) for (*a*) an as-deposited Nb–Zr multi-layer, (*b*) a N_2^+-ion-implanted (5×10^{16} N_2^+ cm^{-2}) Nb–Zr multi-layer and (*c*) Kr^+-ion implanted (5×10^{16} Kr^+ cm^{-2}) Nb–Zr multi-layer: ●, Si + Zr; ○, Zr; ■, Nb; □, C; ▲, N; △, O. The use of sensitivity factors to convert peak-to-peak ratios to absolute concentrations gives rise to some uncertainty mainly in the concentration of gas contaminants.

considered unperturbed, evolves and is different from the equilibrium alloy stoichiometry, resulting in an enriched component which is experimentally known to segregate in that alloy. In this case, Nb was observed in our experiments to segregate at the surface and thus the spike–lattice interface is assumed to be enriched in Nb. Incidentally, Nb segregation, although opposite to predictions of recent theories of surface seg-

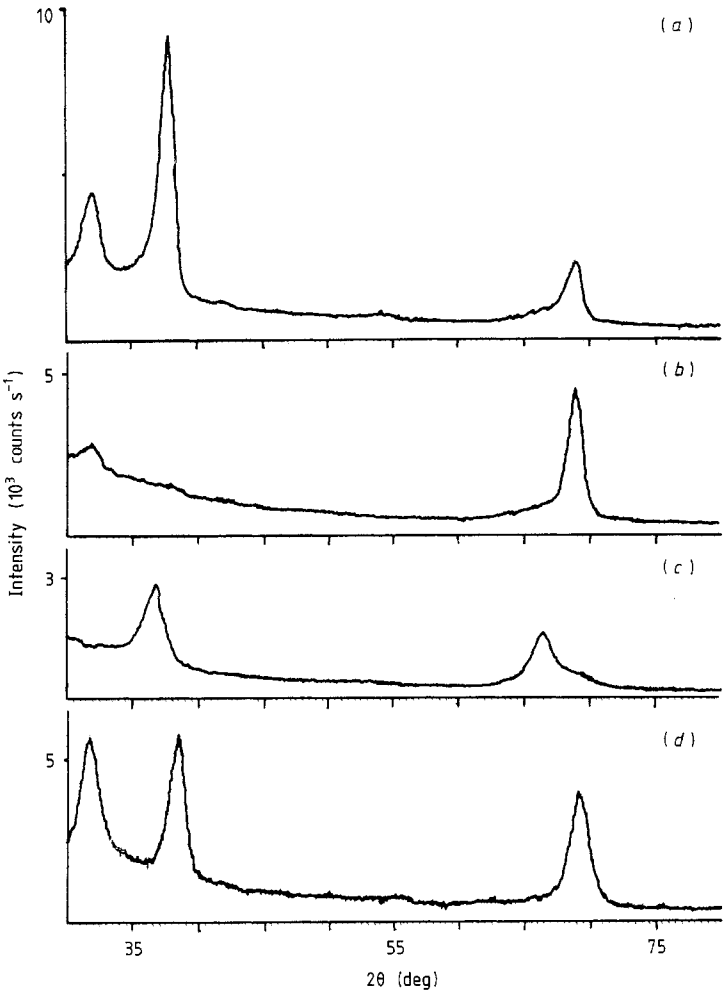

Figure 5. X-ray profiles of the different samples: (*a*) N_2^+-ion-implanted (5×10^{16} N^+ cm^{-2}) Nb–Zr multi-layer; (*b*) Kr^+-ion-implanted (7×10^{15} Kr^+ cm^{-2}) Nb–Zr multi-layer; (*c*) Kr^+-ion-implanted (5×10^{16} Kr^+ cm^{-2}) Nb–Zr multi-layer; (*d*) as-deposited Nb–Zr multi-layer.

regation in binary alloys [17], is in agreement with the reported anomalous Cu segregation in $Cu_{70}Zr_{30}$ [18], again contrasting the usual Zr segregation in transition-metal–Zr alloys. The segregant is assumed to be the electron acceptor from the other element within a charge transfer scheme:

$$\mathrm{Nb}(+1e^-)\,\mathrm{Zr}(-1e^-) \rightarrow (\mathrm{MoY})_e \qquad (1)$$

the letter e indicating the effective atom pair obtained in equation (1). Note that in this case the selection rule on the effectiveness of charge transfer [19] is obeyed.

The 'versus' of charge transfer is in agreement with that predictable on the basis of Pauling's electronegativity values of alloy constituents. The calculated energy change ΔE associated with equation (1) is here positive, $\Delta E = +0.1$ eV, again in agreement with the model, which requires a positive ΔE when the solvent (Nb) segregates; thus it is an electron acceptor. Amorphisation trends in alloys may be predicted on the basis of

Table 1. Critical temperature T_c characteristics of Nb–Zr alloys.

Sample	T_c (K)	ΔT_c (K)	dR/dT ($\Omega\,K^{-1}$)
Co-sputtered crystalline alloy	9.1	0.5	200
Co-sputtered amorphous alloy	[a]	—	—
As-deposited multi-layer	7.4	0.04	1000
Kr^+-ion-implanted glassy multi-layer	4.2	0.08	2500
Kr^+-ion-implanted crystalline multi-layer	[b]	—	—

[a] Transition not observed down to 1 K.
[b] Transition not observed down to 2 K.

Miedema's parameters. The difference between the component electronegativity $\Delta\varphi_o^*$ in the original Nb–Zr and the component electronegativity $\Delta\varphi_e^*$ in effective Mo–Y atom pairs, together with the corresponding difference between the electron density $\Delta n_{WS,o}$ at the boundary of Wigner–Seitz cells in the original Nb–Zr and the electron density $\Delta n_{WS,e}$ at the boundary of Wigner–Seitz cells in effective Mo–Y atom pairs, are calculated. In particular, the direct connection between φ^* and the surface energy γ for any element allows us to consider the quantity

$$\Delta(\Delta\varphi^*) = \Delta\varphi_e^* - \Delta\varphi_o^* \propto (\gamma_{solute} - \gamma_{solvent})_e - (\gamma_{solute} - \gamma_{solvent})_o \qquad (2)$$

as the driving force for producing amorphisation or crystallisation nuclei in the matrix. Indeed, whenever $\Delta(\Delta\varphi^*) < 0$, the difference between the surface energies of effective alloy components is smaller than that between original alloy components. This coincides with a local increase in atomic surface mobility, and thus with a tendency towards lower atomic coordination numbers and high numbers of equivalent configurations. The situation is favourable to glass formation; it is observed in alloys undergoing amorphisation and presenting solvent component segregation. In such a case a high density of metastable effective atom pairs within the matrix is provided which play the role of amorphisation nuclei. Specifically for Nb–Zr, $\Delta(\Delta\varphi^*) = -0.90$ eV and $\Delta(\Delta n_{WS}) = -0.15$.

3. Superconductivity

We measured T_c, the transition width ΔT_c and the slope dR/dT of the resistance against temperature curve in the superconducting transition region, for differently prepared alloys. The results are summarised in table 1 and deserve some comment.

Crystalline films sputtered at room temperature show a T_c-value slightly lower than the highest value reported for bulk crystalline alloys (10.7 K); the difference is attributable first to the sensitivity of T_c to stoichiometry, as our samples are under-stoichiometric in Zr with respect to the observed composition corresponding to the T_c maximum (25 at.% Zr) and secondly to the reduction in T_c induced by gas contaminants, mainly C.

We observe excellent agreement between the data for crystalline multi-layers (T_c = 7.4 K) and the reported value of 7 K for modulated Nb–Zr structures in the limit of high

modulation wavelength (10 nm), comparable with the layer thickness of our samples. T_c was not measured on N_2^+-ion-implanted samples. Indeed, the maintained layer periodicity and crystalline structure make them similar to the as-deposited multi-layers. Also, T_c deteriorations may be inferred owing to implantation damage.

Interface amorphisation upon Kr^+ ion bombardment at rather low doses has the effect of lowering T_c to 4.2 K. Earlier experiments [20] demonstrated that T_c deteriorated after irradiation, although less dramatically than in A15 compounds. In this case, the T_c-value lies near the maximum (5 K) theoretically predicted [21] for amorphous systems with $N_e = 4.8$ as has $Nb_{80}Zr_{20}$; indeed, adjacent positions in the periodic table of alloy components, whose electronic structure differs principally in the occupancy of energy bands, minimises T_c reductions induced by relevant electron redistribution, as should happen with alloy components of highly different valences. Comparing the transition width of unimplanted, and Kr^+-ion-implanted alloys, we note a broadening in the latter case which may be interpreted as a complementary indication of inhomogeneous amorphisation. Glassy regions with maximum disorder are created preferentially in the neighbourhood of the interfaces upon irradiation of the multi-layer; in this case, the mean T_c-value is determined mainly by the proximity effect.

Co-sputtered amorphous alloys rather inexplicably do not present a superconducting transition; the same result is found also for crystalline multi-layers implanted with Kr^+ ions at high doses. A possible explanation of these results lies in the gas contamination which is essential for obtaining amorphous phases in sputtered films, and which was present also in multi-layered samples mixed at high doses. The latter should approach the structure and superconducting behaviour of a defective solid solution $Nb_{80}Zr_{20}$; the dramatic T_c deterioration associated with gaseous impurities [12] is thus confirmed and appears to be independent of the preparation technique.

Our experiments allow us to contribute, although in an indirect fashion, to the debate on the modellisation of superconducting behaviour of transition-metal alloys by reference to the Nb–Zr system—both crystalline and amorphous.

It is generally agreed that the Debye temperature Θ_D of a system presents an intrinsically weak sensitivity to alloy structure and defect concentration, provided that the nature of the chemical bond is preserved. Even the apparently extreme case of crystalline-to-glassy transition, while influencing electron states, does not alter most of the vibrational modes, which are not localised. In particular, possible changes in the density of states may significantly affect only the low-frequency region of the phonon spectrum. Thus we expect that Θ_D-values derived from our T_c data should not result in values very different from those experimentally determined, which lie around $\Theta_D = 205 \pm 6$ K [22] for bulk crystalline specimens of $Nb_{75}Zr_{25}$, and $\Theta_D = 226$ K [3] for Nb–Zr crystalline multi-layers; the pure component values are respectively $\Theta_{Nb} = 275$ K and $\Theta_{Zr} = 292$ K [23].

The Debye temperatures for the different types of sample were derived in the BCS weak-coupling limit; from the equation

$$[\ln(T_c/\Theta_D)_{Nb\text{-}Zr}]^{-1} = C_{Nb}[\ln(T_c/\Theta_D)_{Nb}]^{-1} + C_{Zr}[\ln(T_c/\Theta_D)_{Zr}]^{-1} \qquad (3)$$

where C (at.%) indicates the concentration, we obtain $\Theta_D = 175$ K for Kr^+-ion-implanted amorphous alloys, $\Theta_D = 308$ K for crystalline multi-layers and $\Theta_D = 379$ K for sputtered crystalline alloys. Here we used $T_c = 7.5$ K for pure Nb films, which was measured on samples sputter deposited under the same conditions adopted to prepare alloy films, and $T_c = 3.3$ K for pure Zr [4].

By contrast, from McMillan's strong-coupling limit formula

$$T_c = (\Theta_D/2 \times 1.45)\exp\{-1.04(1 + \lambda_{Nb\text{-}Zr})/[\lambda_{Nb\text{-}Zr} - \mu^*_{Nb\text{-}Zr}(1 + 0.62\lambda_{Nb\text{-}Zr})]\} \qquad (4)$$

with $\lambda_{Nb\text{-}Zr} = 1.3$ [24] and the Coulomb pseudopotential μ^* of the alloy, given by

$\mu^*_{Nb-Zr} = 0.15$ extrapolated from quoted values for the elements [25], $\Theta_D = 120$ K for Kr^+-ion-implanted amorphous alloys, $\Theta_D = 203$ K for crystalline multi-layers and $\Theta_D = 247$ K for sputtered crystalline alloys.

From the comparison between experimental Θ_D data and Θ_D-values obtained from equations (3) and (4), we believe that the effect of disorder on superconductivity in this alloy fits better into a strong-coupling scheme; indeed, this is indicated more on physical grounds in treating the disorder induced in a glassy structure. Also, the Debye temperature of an alloy should not exceed the Θ_D-values of the alloy components.

However, we are aware that there are possible factors which might influence our experimental T_c evaluations and also that, as already mentioned, the Debye temperature is not very sensitive to fine details of the system.

Acknowledgments

One of us (LG) acknowledges funding from Programma Strategico Consiglio Nazionale delle Ricerche Metodologie Cristallografiche Avanzate. The participation of PMO in this research was supported by the Ministero Pubblica Istruzione.

References

[1] Hulm J K and Blaugher R D 1961 *Phys. Rev.* **123** 1569
[2] Abriata J P and Bolcich J C 1982 *Bull. Alloy Phase Diagrams*; 1986 *Binary Alloy Phase Diagrams* vol 2, ed. T B Massalski (Metals Park, OH: American Society for Metal) p 1710
[3] Lowe P W and Geballe T H 1984 *Phys. Rev.* B **29** 4961
[4] Collver M M and Hammond R H 1973 *Phys. Rev. Lett.* **30** 92
[5] Toplicar J R and Finnemore D K 1976 *Solid State Commun.* **19** 859
[6] Toplicar J R and Finnemore D K 1977 *Phys. Rev.* B **16** 2072
[7] Leslie J G, Chen J T and Chen T T 1970 *Can. J. Phys.* **48** 2783
[8] Shull W H and Naugle D F 1977 *Phys. Rev. Lett.* **39** 1580
[9] Tsuei C C, Johnson W L, Laibowitz R B and Viggiano J M 1977 *Solid State Commun.* **24** 615
[10] Hanak J J and Gittlemann J I 1971 *Physica* **55** 555
[11] Poon S J and Carter W L 1980 *Solid State. Commun.* **35** 249
[12] Hauser J J 1985 *Phys. Rev.* B **32** 2887
[13] Cavalleri A, Dapor M, Giacomozzi F, Guzman L, Ossi P M and Scotoni M 1988 *Mater. Sci. Eng.* **99** 201
[14] Singer I L 1984 *Appl. Surf. Sci.* **18** 28
[15] Ossi P M 1989 *Mater. Sci. Eng.* at press
[16] Ossi P M 1988 *Z. Phys.* B **69** 511
[17] Ossi P M 1988 *Surf. Sci.* **201** L519
[18] Vanini F, Büchler St, Yu Xin-nan, Erbudach M, Schlapbach L and Baiker A 1987 *Surf. Sci.* **189–90** 1117
[19] Ossi P M 1985 *Nuovo Cimento* D **5** 1
[20] McEvoy J P Jr and Decell R F 1964 *Appl. Phys. Lett.* **4** 43
[21] Poon S J and Carter W L 1980 *Solid State Commun.* **35** 249
[22] Cappelletti R L, Ginsberg D M and Hulm J K 1967 *Phys. Rev.* **158** 340
[23] Schober H and Dederichs P H 1981 *Landolt–Börnstein New Series* Group III, vol 13a, ed. K-H Hellwege and J L Olsen (Berlin: Springer)
[24] Wolf E L and Noer R J 1979 *Solid State Commun.* **30** 391
[25] Papacostantopoulos D A, Bayer L L, Klein B M, Williams A R, Moruzzi V L and Janak J F 1977 *Phys. Rev.* B **15** 4221